A&A 506, 491–500 (2009)
DOI: 10.1051/0004-6361/200911882

The CoRoT space mission: early results

Astronomy & Astrophysics
Special feature

Planetary transit candidates in Corot-IRa01 field⋆

S. Carpano[1], J. Cabrera[2,3], R. Alonso[4], P. Barge[4], S. Aigrain[6], J.-M. Almenara[7], P. Bordé[8], F. Bouchy[9], L. Carone[10], H. J. Deeg[7], R. De la Reza[11], M. Deleuil[4], R. Dvorak[12], A. Erikson[2], F. Fressin[22], M. Fridlund[1], P. Gondoin[1], T. Guillot[13], A. Hatzes[14], L. Jorda[4], H. Lammer[15], A. Léger[8], A. Llebaria[4], P. Magain[16], C. Moutou[4], A. Ofir[20], M. Ollivier[8], E. Janot-Pacheco[21], M. Pätzold[10], F. Pont[6], D. Queloz[5], H. Rauer[2], C. Régulo[7], S. Renner[2,17,18], D. Rouan[19], B. Samuel[8], J. Schneider[3], and G. Wuchterl[14]

[1] Research and Scientific Support Department, ESTEC/ESA, PO Box 299, 2200 AG Noordwijk, The Netherlands
e-mail: scarpano@rssd.esa.int
[2] Institute of Planetary Research, German Aerospace Center, Rutherfordstrasse 2, 12489 Berlin, Germany
[3] LUTH, Observatoire de Paris, CNRS, Université Paris Diderot, 5 place Jules Janssen, 92190 Meudon, France
[4] Laboratoire d' Astrophysique de Marseille, UMR 6110, 38 rue F. Joliot-Curie, 13388 Marseille, France
[5] Observatoire de Genève, Université de Genève, 51 chemin des Maillettes, 1290 Sauverny, Switzerland
[6] School of Physics, University of Exeter, Stocker Road, Exeter EX4 4QL, UK
[7] Instituto de Astrofísica de Canarias, 38205 La Laguna, Tenerife, Spain
[8] Institut d' Astrophysique Spatiale, Université Paris XI, 91405 Orsay, France
[9] Institut d'Astrophysique de Paris, Université Pierre & Marie Curie, 98bis Bd Arago, 75014 Paris, France
[10] Rheinisches Institut für Umweltforschung an der Universität zu Köln, Aachener Strasse 209, 50931 Köln, Germany
[11] Observatório Nacional, Rio de Janeiro, RJ, Brazil
[12] University of Vienna, Institute of Astronomy, Türkenschanzstr. 17, 1180 Vienna, Austria
[13] Observatoire de la Côte d' Azur, Laboratoire Cassiopée, BP 4229, 06304 Nice Cedex 4, France
[14] Thüringer Landessternwarte, Sternwarte 5, Tautenburg 5, 07778 Tautenburg, Germany
[15] Space Research Institute, Austrian Academy of Science, Schmiedlstr. 6, 8042 Graz, Austria
[16] University of Liège, Allée du 6 août 17, Sart Tilman, Liège 1, Belgium
[17] Laboratoire d'Astronomie de Lille, Université de Lille 1, 1 impasse de l'Observatoire, 59000 Lille, France
[18] Institut de Mécanique Céleste et de Calcul des Ephémérides, UMR 8028 du CNRS, 77 avenue Denfert-Rochereau, 75014 Paris, France
[19] LESIA, Observatoire de Paris-Meudon, 5 place Jules Janssen, 92195 Meudon, France
[20] School of Physics and Astronomy, Raymond and Beverly Sackler Faculty of Exact Sciences, Tel Aviv University, Tel Aviv, Israel
[21] Instituto de Astronomia, Geofísica e Ciências Atmosféricas, Universidade de São Paulo, 05508-900 São Paulo, Brazil
[22] Harvard University, Department of Astronomy, 60 Garden St., MS-16, Cambridge, MA 02138, USA

Received 19 February 2009 / Accepted 27 July 2009

ABSTRACT

Context. CoRoT is a pioneering space mission devoted to the analysis of stellar variability and the photometric detection of extrasolar planets.
Aims. We present the list of planetary transit candidates detected in the first field observed by CoRoT, IRa01, the initial run toward the Galactic anticenter, which lasted for 60 days.
Methods. We analysed 3898 sources in the coloured bands and 5974 in the monochromatic band. Instrumental noise and stellar variability were taken into account using detrending tools before applying various transit search algorithms.
Results. Fifty sources were classified as planetary transit candidates and the most reliable 40 detections were declared targets for follow-up ground-based observations. Two of these targets have so far been confirmed as planets, CoRoT-1b and CoRoT-4b, for which a complete characterization and specific studies were performed.

Key words. stars: planetary systems – techniques: photometric – binaries: eclipsing – planetary systems

1. Introduction

The transit method for detecting exoplanets identifies candidates by monitoring stars for long periods of time, then processing the data to isolate stars that exhibit a periodic flux drop consistent with a Jupiter-sized or smaller companion passing between its parent star and the observer. A large number of targets is necessary, because the probability of a planet producing an observable transit is very low, due to geometric effects. The processing and analysis of gathered data is thus a major undertaking.

⋆ The CoRoT space mission, launched on December 27th 2006, has been developed and is operated by CNES, with contributions from Austria, Belgium, Brazil, ESA, Germany, and Spain. Four French laboratories associated with the CNRS (LESIA, LAM, IAS ,OMP) collaborate with CNES on the satellite development. First CoRoT data are available to the public from the CoRoT archive: http://idoc-corot.ias.u-psud.fr.

The methodology used to analyse thousands of light curves in the search for transiting extrasolar planets was described in detail by Gould et al. (2006) for OGLE data. We summarize here a few concepts:

- CoRoT light curves are processed and filtered for instrumental noise as described in Drummond et al. (2008);
- each of the detection teams applies its own algorithms for detrending the signal (e.g., variability, noise) and searching for planetary transits (see Moutou et al. 2005, 2007);
- the results of each team are combined and each candidate is discussed individually.

In our final discussion, a check is performed to reject clear eclipsing binaries, i.e., systems with lights curves that exhibit secondary eclipses, out-of-transit photometric modulations, and/or events that are too deep to be caused by transiting planets. The shape of transits is also analysed: photometric dips of planets have a "U" shape, while binaries are more "V" shaped. These criteria, however, can only be used for data of with relatively high signal-to-noise ratios. Some examples of eclipsing binary light curves are shown in Figs. 1–3. Raw light curves are shown in the top panel and smoothed, detrended, and folded light curves are shown in the bottom panel. These exhibit the typical features of small secondary eclipses, in phase modulation, and secondary transits out of phase 0.5. Figure 4 shows the raw and folded light curves of a good planetary candidate with a shallow transit (source No. 46, E2 4124, in Tables 2 and 3).

Source confusion with background binaries will also produce false candidates; this is true in particular for CoRoT because of its large PSF (Barge et al. 2008b; Drummond et al. 2008). In this case, one benefits from the three coloured bands of the CoRoT photometric mask. When a candidate is bright enough for its flux to be separated into three bands/colours, the transit is occasionally not observed in one or more of the bands/colours or is a significantly different depth in the separate bands/colours. For the remaining candidates, photometric and/or spectroscopic follow-up are essential to determining of the masses of the system components, by measurements of the radial velocity shift of the spectral lines of the parent star that occur as the planet orbits. In the case of CoRoT, photometric follow-up is useful in cases of source confusion. Spectroscopic ground-based measurements, on the other hand are essential for determinating the masses of the system components, via measurements of the radial velocity shift of the spectral lines of the parent star that occur as the planet orbits.

In this work, we present the results of the joint work of the CoRoT detection teams, a huge effort to separate the wheat from the chaff to provide accurate parameters for the interesting objects. The IRa01 CoRoT data are now public. We offer the fruits of our labor to the astronomical community so it may serve as a starting point for interested researchers. Section 2 contains some details about this initial CoRoT run, including the candidate information from the satellite itself. In Sect. 3, we provide the list of the 50 transiting candidates observed in the first CoRoT field IRa01 and their transit parameters. Results are summarized in Sect. 4.

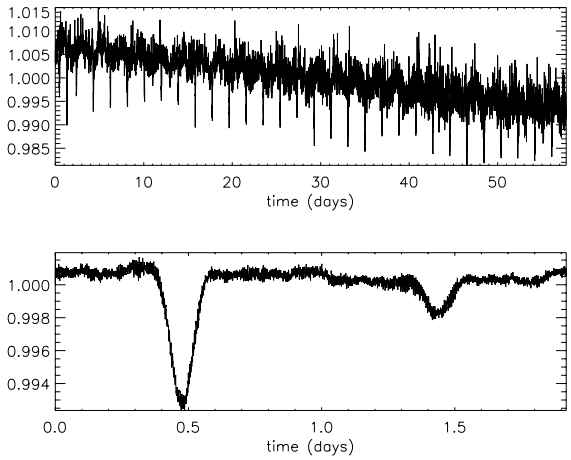

Fig. 1. An eclipsing binary found in IRa01 showing small secondary eclipses. Raw (*top*), smoothed, and detrended folded light curve (*bottom*).

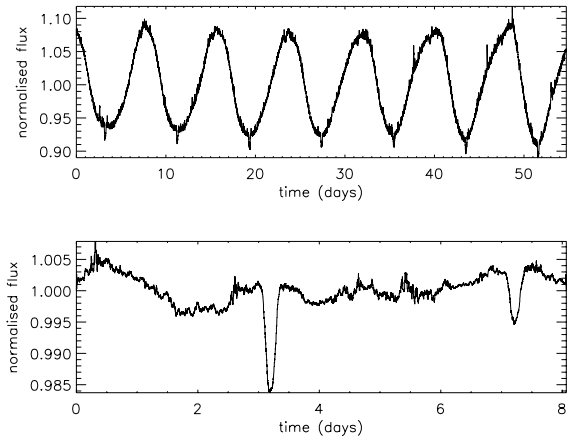

Fig. 2. An eclipsing binary found in IRa01 showing in phase modulation. Raw (*top*), smoothed, and detrended folded light curve (*bottom*).

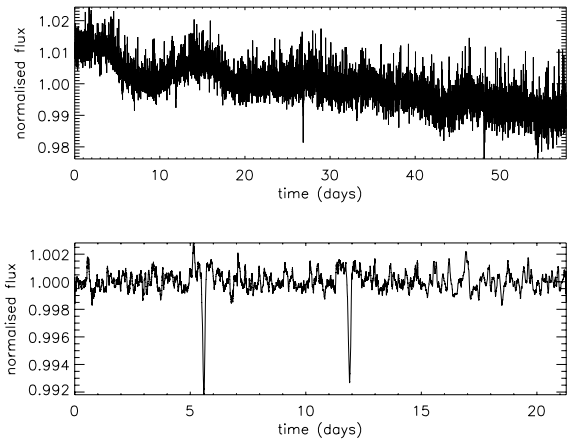

Fig. 3. An eclipsing binary found in IRa01 showing orbital eccentricities. Raw (*top*), smoothed, and detrended folded light curve (*bottom*).

2. CoRoT observations of IRa01 field

CoRoT observed its first field from early February 2008 until early April, for approximatively 60 days. The run code "IRa01" is explained as following. The "IR" means "initial run" in contrast to the subsequent "long runs" (LR) and "short runs" (SR). The third letter refers to the direction with respect to the Galactic center ("a", as in this case, anticenter or "c" Galactic center). The last two digits are the sequence for this type of observation (01 being the first one).

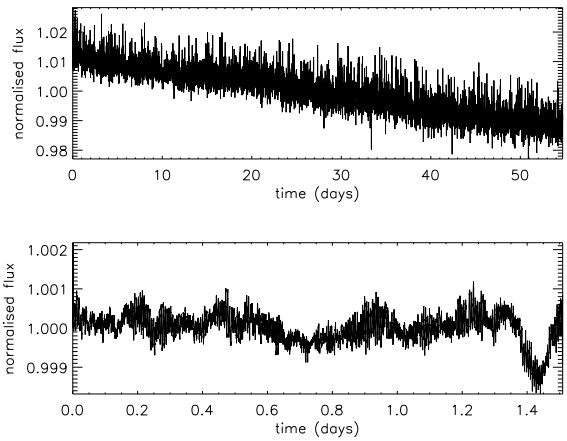

Fig. 4. Raw and folded light curve of a planetary candidate (source No. 46, E2 4124).

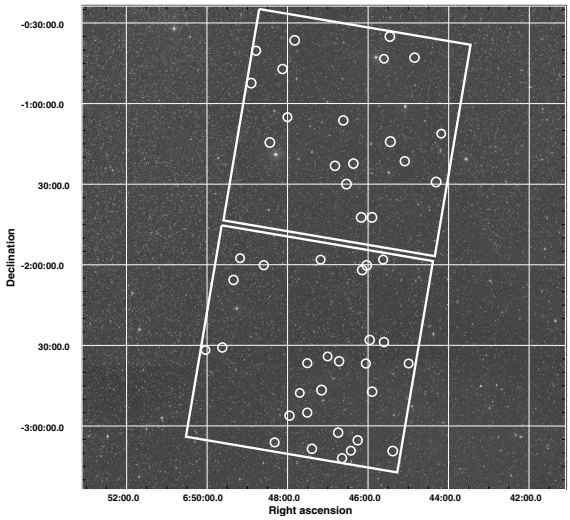

Fig. 5. DSS image of the sky observed by CoRoT during the IRa01. Overlaid are the positions of the 50 planetary transit candidates and the portion of the field covered by the 2 exoplanets CCD.

Table 1. List of the detection teams (institutes and people).

Team	Participants
DLR	Heike Rauer, Anders Erikson, Stefan Renner
ESTEC	Malcolm Fridlund, Stefania Carpano
Exeter	Suzanne Aigrain, Frédéric Pont, Aude Alapini
IAC	Hans Deeg, José M. Almenara, Clara Régulo
IAS	Pascal Bordé, Benjamin Samuel
Köln	Martin Pätzold, Ludmilla Carone
LAM	Pierre Barge, Roi Alonso
LUTh	Jean Schneider, Juan Cabrera

3898 sources were observed in IRa01 using coloured filters (B, V, R colours), while 5974 sources were monitored at a single monochromatic band. To analyse these data sets, detection teams were established in a number of different collaborating institutes. Their task is to provide a list of candidates, their ranking (according to the probability of their planetary nature), as well as a first estimate of transit ephemerides and parameters. At this point, 8 teams are participating, each using their own independently-developed detection methods. Table 1 contains a list of the different institutions involved and the names of the contributors. Some of these methods were presented during a pre-launch performance simulation described in Moutou et al. (2005), while others have been or will be developed in separated papers (i.e., Carpano & Fridlund 2008; Renner et al. 2008; Régulo et al. 2007). The algorithms described in these works are generally based on the following fundamental approaches: correlation with sliding transit template, box-shaped signal search, box-fitting least-squares (BLS), wavelet transformation, or Gaussian fitting of folded light curve. A merged list of 92 planetary transit candidates was compiled by the teams, which was reduced to a final list of 50 candidates after discussion (most of the other 42 candidates were classified as binaries). The 40 most robust candidates were recommended for ground-based follow-up, the results of which are reported in Moutou et al. (2009). Two planets from the final list of 40 candidates, CoRoT-1b and CoRoT-4b, have so far been confirmed as planets. More details about the discovery of these two planets can be found in Barge et al. (2008a) and Aigrain et al. (2008), respectively.

Figure 5 shows the sky coverage of the 2 CCDs dedicated to exoplanetary science and the positions of the candidates within this field of view. Table 2 provides a list of planetary candidates in the IRa01 field, including their CoRoT- and window-ID numbers, J2000 positions, an indication of whether the candidate was observed in three colours ("CHR") or monochrome ("MON"), magnitude(s), and exposure times (in s). A change in the time sampling from 512 s to 32 s indicates that several transits were detected in the first portion of the light curve and the Alarm Mode (Quentin et al. 2006; Surace et al. 2008) was chosen to resample those targets to improve the time accuracy. All parameters derived from the Exo-Dat database (Meunier et al. 2007; Deleuil et al. 2009) .

3. Compiling a list of candidates with their transit parameters

The selection process of planetary candidates for follow-up has several steps. First, each detection team analyses the tens of thousands of light curves independently using their own filtering and detection codes. A list of candidates is compiled by each team, and arranged in order of a numerical priority from 1 for the best candidates to 3 or 4 for doubtful sources (e.g., "V" shaped transit, suspicion of secondary transits, noisy data, mono-transits). A "B" is given for binary sources. All lists are then merged into a single list, where the sources at the top level are the candidates found by several teams at high priorities. The teams interact regularly by means of weekly teleconferences. Apart from most likely candidates and the binaries, all sources are rediscussed and reanalysed. The list of transit candidates selected by the detection teams and sorted by the probability of their planetary nature of highest probability is then examined by the follow-up teams. They are responsible for confirming (or rejecting) the planetary nature of each candidate by ground-based observations. They focus primarily on the candidates of highest priorities, although stellar magnitude and amount of observing time available will influence their final decisions.

The transit parameters of the candidates were estimated as follows. First, a low-order polynomial was fit to the regions around each transit in an attempt to normalise the data. A first estimate of the period and epoch are used to phase-fold the light curve. The data points are binned, errors being assigned according to the standard deviation of the points inside each bin divided by the square-root of the number of points in each bin.

Table 2. List of the 50 planetary transit candidates detected in the CoRoT IRa01 field, see text for more details.

No.	CoRoT-ID	Win-ID	Right ascension, declination	Exo-Dat *R* mag	Colour	Time Sampling
1	0102723949	E1 2046	6:44:11.03943,–1:11:13.236	13.60	CHR	512
2	0102729260	E1 1319	6:44:18.72070,–1:29:11.328	14.77	CHR	512
3	0102763847	E1 1158	6:45: 5.28076,–1:21:25.236	13.11	CHR	512, 32
4	0102787048	E1 0288	6:45:36.24023,–0:43:17.400	13.17	CHR	512, 32
5	0102787204	E2 3787	6:45:36.48010,–2:28:50.664	14.00	CHR	512
6	0102798247	E2 1857	6:45:53.99963,–2:47:15.900	14.06	CHR	512, 32
7	0102806520	E1 4591	6:46:10.31982,–1:42:23.688	13.70	CHR	512
8	0102809071	E2 1136	6:46:15.36072,–3: 5:19.608	13.20	CHR	512, 32
9	0102815260	E2 2430	6:46:25.68054,–3: 9:13.284	14.57	CHR	512, 32
10	0102825481	E2 0203	6:46:43.20007,–2:35:58.308	13.07	CHR	512, 32
11	0102826302	E2 1712	6:46:44.63928,–3: 2:32.208	13.98	CHR	512, 32
12	0102829121	E1 0399	6:46:49.44031,–1:23:11.616	13.66	CHR	512
13	0102855534	E2 1736	6:47:30.47974,–2:55: 4.116	13.85	CHR	512, 32
14	0102856307	E1 0396	6:47:31.68091,–1:23:26.808	13.58	CHR	512
15	0102874481	E2 1677	6:47:57.11975,–2:56:10.896	13.84	CHR	512
16	0102890318	E2 1126	6:48:19.20044,–3: 6: 7.776	13.43	CHR	512, 32
17	0102895957	E1 0783	6:48:26.40015,–1:14:31.344	12.72	CHR	512, 32
18	0102912369	E1 0330	6:48:46.79993,–0:40:21.972	13.45	CHR	512, 32
19	0102918586	E1 2755	6:48:54.23950,–0:52:22.800	12.24	CHR	512, 32
20	0102753331	E1 4617	6:44:50.87952,–0:42:53.280	15.87	MON	512
21	0102759638	E2 3724	6:44:59.52026,–2:36:45.144	14.79	MON	512
22	0102777119	E2 4290	6:45:23.04016,–3: 9:23.688	15.03	MON	512
23	0102779966	E1 4108	6:45:26.87988,–1:14: 9.456	14.94	MON	512
24	0102780627	E1 1531	6:45:27.83936,–0:35: 4.668	14.98	MON	512
25	0102788073	E2 2009	6:45:37.67944,–1:58: 9.300	14.18	MON	512
26	0102798429	E1 2774	6:45:54.23950,–1:42:22.752	15.52	MON	512
27	0102800106	E2 3010	6:45:57.59949,–2:28: 0.732	15.49	MON	512
28	0102802430	E2 4300	6:46: 2.16064,–2: 0:13.428	14.33	MON	512
29	0102802996	E2 3150	6:46: 3.35999,–2:36:46.548	14.96	MON	512
30	0102805893	E2 2604	6:46: 8.88062,–2: 2: 0.348	15.42	MON	512
31	0102812861	E1 2648	6:46:21.84082,–1:22:19.128	15.59	MON	512
32	0102819021	E1 2328	6:46:32.16064,–1:29:58.812	15.10	MON	512
33	0102821773	E1 4998	6:46:36.95984,–1: 6:15.768	15.48	MON	512
34	0102822869	E2 4058	6:46:38.88062,–3:12: 4.860	15.55	MON	512
35	0102835817	E2 3425	6:47: 0.23987,–2:34: 7.140	15.60	MON	512
36	0102841669	E2 3854	6:47: 9.36035,–2:46:39.108	14.91	MON	512
37	0102842120	E2 3952	6:47:10.07996,–2:57: 1.944	13.98	MON	512
38	0102842459	E2 1407	6:47:10.79956,–1:58: 7.356	14.77	MON	512
39	0102850921	E2 2721	6:47:23.75977,–3: 8:32.424	12.90	MON	512
40	0102855472	E2 0704	6:47:30.47974,–2:36:40.140	13.86	MON	512
41	0102863810	E2 4073	6:47:42.00073,–2:47:43.404	15.39	MON	512
42	0102869286	E1 2329	6:47:49.44031,–0:36:29.052	15.52	MON	512
43	0102876631	E1 3336	6:48: 0.23987,–1: 5: 5.964	14.56	MON	512
44	0102881832	E1 4911	6:48: 7.43958,–0:47: 9.024	15.05	MON	512
45	0102903238	E2 4339	6:48:35.52063,–2: 0:12.096	15.61	MON	512
46	0102926194	E2 4124	6:49: 3.59985,–2:48:34.488	15.73	MON	512
47	0102932089	E2 3819	6:49:10.79956,–1:57:34.452	16.00	MON	512
48	0102940315	E2 4467	6:49:20.63965,–2: 5:37.716	15.81	MON	512
49	0102954464	E2 3856	6:49:37.43958,–2:30:49.140	15.97	MON	512
50	0102973379	E2 1063	6:50: 2.40051,–2:31:47.604	14.09	MON	512

A Levenberg-Marquardt algorithm (Levenberg 1944; Marquardt 1963) is used to fit a trapezoid (where its center, depth, duration, and time of ingress are the fit parameters) to the phase-folded curve. The best-fit model trapezoid is then cross-correlated at each individual transit in the light curve, to determine their centers. A linear fit to the resulting O−C diagram refines the estimations of the period and epoch. With this new ephemeris, the process is iterated, until the ephemerides are within the error bars of the previous values (typically one iteration is sufficient). The error in both the period and epoch are the formal errors in the linear fit.

Table 3 lists the transit parameters for the 50 planetary candidates: identifiers, coordinates, periods, and epochs with their associated errors, the transit duration (in hours) and depth (in %), and an estimate of the stellar density inferred by the transit light curve fit as explained in Seager & Mallén-Ornelas (2003). This parameter combined with the other characteristics of the candidates (e.g., depth, duration, shape, out of transit modulation, stellar parameters) are used as input for the ranking of candidates given to the follow-up team. We note that the light curve of the candidate 37 is contaminated with the curve of a clear eclipsing binary (source 97 in Table A.1). The value of its transit parameters may therefore have been affected.

Table 3. Transit parameters of the 50 planetary candidates.

No.	Win-ID	Period (d)	Error period (d)	Epoch (d) +2 454 000	Error epoch (d)	Duration (h)	Depth	Density ($\rho_\odot$)
1	E1 2046	–	–	167.9153	2.1E-03	5.638	1.2E-02	–
2	E1 1319	1.69851	2.6E-05	136.4886	8.5E-04	2.335	4.4E-03	0.5374
3	E1 1158	10.53096	1.3E-04	140.0856	3.3E-04	2.159	1.4E-02	8.9253
4	E1 0288	7.89296	4.6E-04	135.0691	2.3E-03	4.512	3.7E-03	0.3740
5	E2 3787	0.85809	3.9E-06	138.1467	1.4E-04	2.660	1.3E-03	0.1955
6	E2 1857	0.82169	1.4E-05	138.3168	6.6E-04	1.829	4.7E-03	0.8132
7	E1 4591	4.29539	3.5E-05	136.6231	2.6E-04	2.295	2.9E-03	1.0074
8	E2 1136	1.22387	3.4E-06	139.2401	1.3E-04	2.748	1.8E-03	0.2076
9	E2 2430	3.58747	9.2E-05	139.2341	8.4E-04	5.570	1.2E-02	0.5040
10	E2 0203	5.16868	1.9E-05	138.7811	1.2E-04	2.918	3.4E-02	5.3662
11	E2 1712	2.76741	5.8E-05	139.6140	5.3E-04	4.114	2.4E-03	0.6866
12	E1 0399	33.06200	3.5E-03	151.7875	2.2E-03	3.015	1.5E-02	11.0820
13	E2 1736	21.72025	1.5E-03	144.2915	2.8E-03	13.175	1.2E-02	0.1613
14	E1 0396	7.82394	6.9E-04	140.0779	2.7E-03	2.788	8.2E-04	0.6066
15	E2 1677	–	–	156.8022	1.2E-03	6.795	3.0E-02	–
16	E2 1126	1.50900	1.2E-05	138.3265	3.3E-04	2.450	2.2E-02	2.7151
17	E1 0783	–	–	162.9538	1.3E-03	5.498	6.4E-03	–
18	E1 0330	9.20191	3.4E-04	141.3652	1.3E-03	4.404	1.2E-02	3.1234
19	E1 2755	4.39125	4.2E-05	139.3811	3.9E-04	2.486	2.4E-02	3.8575
20	E1 4617	19.75581	3.8E-03	143.8531	3.1E-03	16.595	4.0E-02	0.1324
21	E2 3724	12.32616	1.4E-03	142.4015	2.7E-03	11.802	1.0E-02	0.1094
22	E2 4290	2.20546	1.5E-05	139.6775	2.1E-04	8.741	4.0E-03	0.0307
23	E1 4108	7.36644	8.4E-04	137.9420	2.7E-03	2.911	5.2E-03	1.6112
24	E1 1531	2.38147	6.7E-05	137.2002	8.8E-04	2.160	1.2E-02	2.0203
25	E2 2009	10.84581	1.4E-03	141.7762	2.9E-03	5.040	4.1E-03	0.2817
26	E1 2774	1.60551	5.9E-05	135.8954	1.3E-03	3.214	7.2E-03	0.3168
27	E2 3010	23.20918	6.1E-03	159.0750	2.6E-03	3.182	1.7E-02	9.3127
28	E2 4300	5.80656	3.7E-04	139.0526	1.6E-03	3.236	5.1E-03	0.8538
29	E2 3150	–	–	163.4256	2.1E-03	4.041	1.7E-02	–
30	E2 2604	3.81967	1.4E-04	138.2163	1.3E-03	4.366	2.5E-03	0.2051
31	E1 2648	3.68241	2.5E-04	138.4929	1.8E-03	3.138	8.8E-03	0.7965
32	E1 2328	4.50975	3.1E-04	137.6290	2.1E-03	5.911	6.8E-03	0.1238
33	E1 4998	10.08309	1.1E-03	142.3704	2.6E-03	2.787	1.9E-02	5.6972
34	E2 4058	–	–	188.9298	4.2E-03	3.651	9.3E-03	–
35	E2 3425	1.18553	3.0E-05	139.2383	9.1E-04	2.996	3.6E-03	0.2295
36	E2 3854	1.14181	3.0E-05	138.9064	7.4E-04	1.971	1.4E-03	1.4261
37	E2 3952	13.47756	4.1E-03	160.6192	3.2E-03	2.605	2.2E-03	7.4800
38	E2 1407	5.16776	3.2E-04	140.9219	1.8E-03	1.604	2.5E-02	16.2410
39	E2 2721	0.61161	6.9E-06	138.5715	3.5E-04	2.569	6.0E-03	0.4197
40	E2 0704	2.15520	6.1E-05	139.2776	7.9E-04	5.891	7.2E-03	0.1898
41	E2 4073	15.00128	1.3E-03	140.1756	2.4E-03	5.347	3.9E-02	2.7669
42	E1 2329	1.86725	5.6E-05	135.5561	5.8E-04	2.636	3.7E-03	0.4757
43	E1 3336	1.38972	3.3E-05	135.8757	7.7E-04	2.751	1.7E-03	0.2017
44	E1 4911	2.16638	8.7E-05	136.5974	1.3E-03	5.891	9.6E-03	0.1008
45	E2 4339	1.36204	3.9E-05	139.1842	9.9E-04	2.220	1.7E-03	0.3215
46	E2 4124	1.50872	7.0E-05	139.5222	1.3E-03	3.350	2.1E-03	0.1436
47	E2 3819	1.56554	4.7E-05	138.7047	8.6E-04	3.204	2.1E-02	0.6651
48	E2 4467	16.44935	2.2E-03	140.8322	3.0E-03	5.527	1.4E-02	0.9068
49	E2 3856	16.56276	1.7E-03	145.6439	2.7E-03	1.482	2.1E-02	70.9060
50	E2 1063	–	–	171.7411	1.5E-03	8.554	7.7E-03	–

Figure 6 shows the transit depth versus orbital period for all sources in IRa01 including planetary candidates and stellar binaries. There does not seem to be any correlation between transit depth and period, for periods below 10 days. The correlation of the depth with the number of observed transits is evident for period >10 days. We note that several mono-transits have also been reported. This suggests that the detection methods used by the detection teams do not strongly depend on the number of transits as long as several are detectable. A detailed study of the capabilities of the detection algorithms is currently ongoing.

Figure 7 shows the same diagram but for the transit depth versus the V magnitude. There is again no strong dependence between these two parameters that is apparent for magnitudes brighter than 16, a slight dependence is however evident for fainter stars. This might indicate that the noise is not dominated by photon noise but rather by instrumental effects, including hot pixels (see Fig. 8).

Hot pixels are characterized by sudden jumps in the light curve, followed either by an exponential or sudden decay. They are caused by high-energy particle impacts, mainly protons, on the detector. A description of the radiation effects on the CoRoT CCD can be found in Pinheiro da Silva et al. (2008). The number of hot pixels of intensity higher than a certain quantity of electrons at the beginning of the first 5 CoRoT runs (IRa01, SRc01,

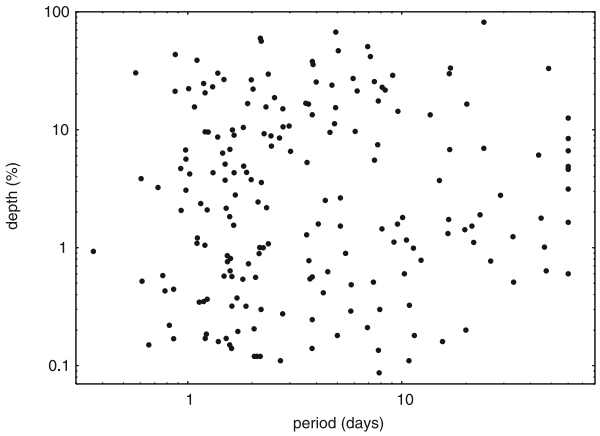

Fig. 6. Transit depth versus orbital period for all sources with detected transits (planetary candidates and clear stellar binaries).

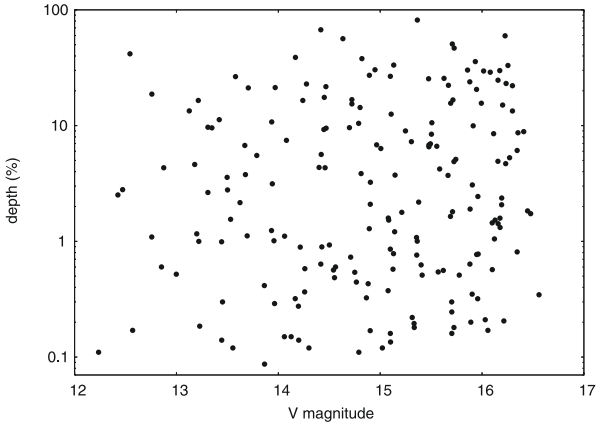

Fig. 7. Transit depth versus V magnitude for all sources with detected transits (planetary candidates and clear stellar binaries).

LRc01, LRa01, and SRa01) are shown by Auvergne et al. (2009) in their Fig. 6. In the case of the initial run, about 26 700, 3200, and 24 bright pixels were reported with an intensity of electrons higher than 300 e^-, 1000 e^-, and 10000 e^-, respectively. No efficient filtering method has so far been found that is capable of removing these sudden jumps/decays from the light curves while leaving the transits intact. The detection teams deal with them mainly by renormalising the light curve before and after the jumps and leaving a gap at the place of the discontinuities. Replacing hot pixel events with short gaps avoids the detection of spurious signals without having a large impact on the detected transits.

A study of the noise properties was performed by Aigrain et al. (2009). They claim that, after pre-processing of the light curves to minimize long-term variations and outliers, the behaviour of the noise on a 2h timescale is close to pre-launch specification. However, a noise level of a factor 2−3 above the photon noise is still found because of the residual jitter noise and hot pixel events. Furthermore, there is evidence of a slight degradation in the performance over time for the first 3 long runs (IRa01, LRc01, and LRa01).

The transit detection threshold is discussed in Moutou et al. (2009), following the model described in Pont et al. (2006). In Moutou et al. (2009), they examine the location of planet candidates in the magnitude versus transit signal ($dn^{0.5}$, where d is the transit depth and n is the number of points in the transit). They find that the detection threshold does not

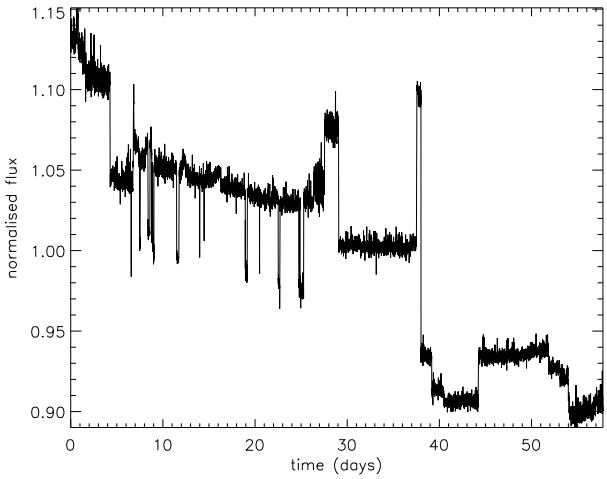

Fig. 8. Typical light curve containing frequent jumps caused by "hot pixels".

depend on magnitude and conclude that correlated fluctuations (instrumental effects or stellar variability) dominates, which is similar to what we conclude from Fig. 7. The detection limit is at $dn^{0.5} = 0.009$, substantially higher than in the pre-launch models.

The implications of these noise properties and detection threshold on planet detection are discussed in Fressin et al. (in prep.). They use the CoRoTlux transit survey simulator described in Fressin et al. (2007) to show that the CoRoT yield on the first 4 fields is less than one-half that expected. This gap will probably be reduced as the follow-up of CoRoT candidates nears completion. Fressin et al. (2007) provides an estimate of the planet occurrence in close orbit around F-G-K dwarf stars as a function of the radius of the planet, which agrees with radial velocity, ground-based transit, and CoRoT discoveries. Interestingly, they show that CoRoT's detection of one Super-Earth (i.e., CoRoT-7b, see Léger et al. 2009) agrees with the high expectations from the HARPS team for the number of close-in Super-Earths (i.e., for 30% of main-sequence dwarfs – see Lovis et al. 2009), because this kind of planets typically needs to have a bright K dwarf host to exceed the CoRoT detection threshold.

4. Summary

CoRoT has observed its first star field, IRa01, for 2 months since the beginning of 2008. It has obtained light curves of 3898 chromatic sources and 5974 monochromatic sources, which have been analysed by the detection teams. About one hundred sources have been classified as potential candidates and 50 of them have been kept as good candidates. The transit parameters of these candidates are listed in Table 3. About 40 of these should be followed-up with ground-based facilities. So far only two planets, CoRoT-1b and CoRoT-4b, have been confirmed, from IRa01, each published individually as the subject of a dedicated study. We provide in the Appendix a list of eclipsing binaries found in the field.

References

Aigrain, S., Collier Cameron, A., Ollivier, M., et al. 2008, A&A, 488, L43
Aigrain, S., Pont, F., Fressin, F., et al. 2009, A&A, 506, 425

Auvergne, M., Bodin, P., Boisnard, L., et al. 2009, A&A, 506, 411
Barge, P., Baglin, A., Auvergne, M., et al. 2008a, A&A, 482, L17
Barge, P., Baglin, A., Auvergne, M., & the CoRoT team. 2008b, in IAU Symp., 249, 3
Carpano, S., & Fridlund, M. 2008, A&A, 485, 607
Deleuil, M., Meunier, J., Moutou, C., et al. 2009, AJ, 138, 649
Drummond, R., Lapeyrere, V., Auvergne, M., et al. 2008, A&A, 487, 1209
Fressin, F., Guillot, T., Morello, V., & Pont, F. 2007, A&A, 475, 729
Gould, A., Dorsher, S., Gaudi, B. S., & Udalski, A. 2006, Acta Astron., 56, 1
Kabath, P., Eigmüller, P., Erikson, A., et al. 2007, AJ, 134, 1560
Léger, A., Rouan, D., Schneider, J., et al. 2009, A&A, 506, 287
Levenberg, K. 1944, The Quarterly of Applied Mathematics, 2, 164
Lovis, C., Mayor, M., Bouchy, F., et al. 2009, in IAU Symp., 253, 502
Marquardt, D. 1963, SIAM J. Appl. Math., 11, 431
Meunier, J.-C., Deleuil, M., Moutou, C., et al. 2007, in Astronomical Data Analysis Software and Systems XVI, ed. R. A. Shaw, F. Hill, & D. J. Bell, ASP Conf. Ser., 376, 339
Moutou, C., Pont, F., Barge, P., et al. 2005, A&A, 437, 355
Moutou, C., Aigrain, S., Almenara, J., et al. 2007, in Transiting Extrapolar Planets Workshop, ed. C. Afonso, D. Weldrake, & T. Henning, ASP Conf. Ser., 366, 127
Moutou, C., Pont, F., Bouchy, F., et al. 2009, A&A, 506, 321
Pinheiro da Silva, L., Rolland, G., Lapeyrere, V., & Auvergne, M. 2008, MNRAS, 384, 1337
Pont, F., Zucker, S., & Queloz, D. 2006, MNRAS, 373, 231
Quentin, C. G., Barge, P., Cautain, R., et al. 2006, in ESA SP, ed. M. Fridlund, A. Baglin, J. Lochard, & L. Conroy, ESA SP, 1306, 409
Régulo, C., Almenara, J. M., Alonso, R., Deeg, H., & Roca Cortés, T. 2007, A&A, 467, 1345
Renner, S., Rauer, H., Erikson, A., et al. 2008, A&A, 492, 617
Seager, S., & Mallén-Ornelas, G. 2003, ApJ, 585, 1038
Surace, C., Alonso, R., Barge, P., et al. 2008, SPIE Conf. Ser., 7019

Appendix A: Binary stars in CoRoT IRa01 field

Table A.1 lists of all eclipsing binaries that have been identified in CoRoT-IRa01 field. Five of these sources (No. 4, 32, 34, 97, 123) were reported in Kabath et al. (2007) within their Berlin Exoplanet Search Telescope (BEST) survey of variable stars in the CoRoT fields. Sources 1 to 139 are ordinary eclipsing binaries (note that sources labeled 39 and 40 are two binaries in the same mask of CoRoT, so there is a single CoRoT identifier for both), whereas sources 140 to 145 are eclipsing binaries where only one eclipse has been found, so their period could not be determined (these are the so-called mono-transit events).

Table A.1. Eclipsing binary candidates found in IRa01.

No.	CoRoT-ID	Win-ID	Alpha (°)	Delta (°)	*V* Mag	Period (d)	Epoch (d) +2 454 000	Dur. (h)	Depth (%)
1	102759638	E2 3724	101.248	−2.61254	15.13	12.32900 ± 1.00E-03	142.39700 ± 1.59E-01	11.440	0.800
2	102781577	E2 3479	101.371	−2.93473	15.33	5.00429 ± 1.61E-02	141.17440 ± 1.17E-01	7.200	0.300
3	102819749	E2 1568	101.639	−2.59904	15.11	36.92300 ± 1.00E-03	162.36000 ± 1.00E-02	7.300	13.000
4	102941623	E2 2199	102.343	−2.17165	15.31	1.65060 ± 3.00E-04	138.99400 ± 3.00E-03	5.900	0.270
5	102707895	E1 1873	100.951	−0.96872	13.96	5.78390 ± 5.00E-04	136.85500 ± 8.00E-03	9.450	0.430
6	102765395	E2 4693	101.280	−2.31180	15.88	1.57651 ± 4.72E-04	139.71463 ± 7.22E-03	1.730	0.630
7	102855348	E1 0081	101.876	−1.20972	12.23	5.42500 ± 2.50E-03	136.77300 ± 1.30E-02	3.000	0.170
8	102823343	E1 4238	101.665	−1.81256	15.57	7.44690 ± 1.30E-03	138.54600 ± 2.00E-03	3.620	6.800
9	102771473	E2 4752	101.315	−2.24456	16.56	1.13230 ± 2.46E-04	139.37964 ± 8.25E-03	2.390	0.480
10	102826074	E1 4597	101.684	−1.32652	16.25	48.57814 ± 2.87E-03	140.23557 ± 1.87E-03	10.310	15.620
11	102725806	E1 1875	101.057	−1.58770	15.42	0.34180 ± 1.00E-04	136.02320 ± 2.92E-03	0.000	8.230
12	102739450	E1 2209	101.135	−0.64769	15.62	2.07265 ± 1.00E-05	136.16830 ± 6.83E-03	0.560	2.820
13	102760888	E1 4417	101.255	−1.70619	13.44	1.90450 ± 1.90E-04	136.09635 ± 3.20E-03	2.020	0.160
14	102791304	E2 4439	101.426	−3.11075	16.30	13.57800 ± 1.00E-03	149.71745 ± 7.30E-04	25.200	49.000
15	102794063	E2 3276	101.442	−2.80939	16.35	0.38194 ± 5.00E-05	138.34893 ± 1.00E-04	3.720	20.400
16	102794135	E1 0736	101.442	−1.85562	14.63	0.26387 ± 5.00E-05	135.10625 ± 1.00E-04	1.710	5.760
17	102798366	E1 1488	101.476	−1.25857	15.29	0.39568 ± 5.00E-05	135.47506 ± 1.00E-04	3.710	1.830
18	102806220	E2 3454	101.540	−2.47491	15.92	0.34973 ± 5.00E-04	138.58722 ± 1.00E-04	3.700	35.000
19	102806409	E2 4376	101.542	−3.14874	16.09	0.64735 ± 5.00E-04	138.54850 ± 1.00E-04	3.300	20.100
20	102808511	E2 0968	101.560	−2.37561	13.37	0.23966 ± 5.00E-04	138.22310 ± 1.00E-04	2.600	31.100
21	102814334	E1 1671	101.601	−1.59656	14.12	0.65776 ± 5.00E-04	135.76000 ± 1.00E-02	3.300	0.190
22	102819924	E2 4711	101.640	−2.92284	16.17	16.70000 ± 3.00E-03	149.65103 ± 2.60E-03	26.100	47.800
23	102821683	E2 2608	101.653	−2.17193	14.75	1.81094 ± 3.80E-04	140.03110 ± 8.30E-03	18.700	2.110
24	102822723	E2 2726	101.661	−2.26234	14.93	10.12150 ± 3.55E-04	144.23984 ± 8.50E-04	11.200	30.400
25	102826085	E2 0778	101.684	−2.24207	13.01	1.02583 ± 7.00E-05	138.88381 ± 2.07E-03	10.500	5.100
26	102846142	E1 1128	101.819	−1.45863	15.04	0.41086 ± 5.00E-04	135.05939 ± 1.00E-04	4.600	14.500
27	102870524	E1 2045	101.963	−1.48052	14.13	1.86800 ± 1.00E-03	136.47937 ± 1.00E-03	1.100	0.270
28	102888076	E2 3346	102.068	−2.53040	15.37	24.19210 ± 2.72E-03	142.60754 ± 3.00E-03	5.900	34.100
29	102897917	E1 4302	102.120	−0.72015	16.13	0.44560 ± 5.00E-04	135.27050 ± 1.00E-04	4.400	20.700
30	102904593	E1 1080	102.154	−0.60466	15.13	16.89607 ± 2.94E-04	142.04979 ± 3.40E-04	5.500	17.900
31	102910432	E2 1277	102.185	−2.62631	14.87	0.31221 ± 5.00E-04	138.56415 ± 1.00E-04	3.400	4.710
32	102924081	E2 0262	102.254	−1.89538	12.27	0.37350 ± 1.00E-04	138.25600 ± 1.00E-04	4.000	24.100
33	102939944	E2 0738	102.334	−2.10704	14.36	0.87378 ± 5.00E-04	139.04790 ± 5.00E-03	2.200	0.240
34	102940723	E2 1704	102.338	−2.11356	11.73	0.87407 ± 5.00E-04	138.17630 ± 5.00E-03	3.100	43.600
35	102943300	E2 0915	102.351	−2.32753	13.21	20.13885 ± 7.83E-03	153.57863 ± 5.70E-03	16.100	25.100
36	102961901	E2 2711	102.443	−2.01828	15.81	0.42090 ± 1.00E-04	138.30993 ± 5.00E-04	4.300	30.500
37	102844383	E1 1495	101.808	−1.33584	15.10	1.52718 ± 4.85E-04	135.45534 ± 5.00E-04	2.400	1.100
38	102846496	E2 2095	101.821	−3.11782	14.77	0.85681 ± 5.00E-04	138.40500 ± 5.00E-04	1.800	0.430
39	102842572	E2 2746	101.795	−2.05667	15.91	4.00256 ± 5.00E-04	138.17830 ± 5.00E-04	3.300	9.900
40	–	–	–	–	–	2.46350 ± 5.00E-04	139.19670 ± 5.00E-04	2.500	2.700
41	102745492	E1 4732	101.168	−1.12118	16.27	3.60467 ± 7.64E-04	138.95489 ± 7.50E-03	2.472	5.285
42	102901962	E1 3608	102.141	−1.68750	16.41	2.44483 ± 5.17E-03	137.09217 ± 4.55E-02	4.174	8.865
43	102912741	E2 0254	102.196	−2.89809	13.35	1.24542 ± 8.90E-05	138.51084 ± 2.27E-03	2.117	9.565
44	102817472	E2 1390	101.623	−2.75731	15.13	1.47876 ± 3.48E-04	138.57094 ± 7.04E-03	4.702	0.575
45	102846132	E2 3660	101.819	−2.49772	16.35	1.38144 ± 5.24E-04	139.38388 ± 6.70E-03	4.487	8.665
46	102853429	E2 1218	101.865	−2.79528	13.53	1.63806 ± 1.16E-04	138.50031 ± 2.21E-03	3.141	1.550
47	102879429	E1 1827	102.018	−1.57061	15.48	4.03054 ± 6.90E-05	137.84405 ± 1.12E-03	2.872	6.560
48	102982347	E2 1745	102.563	−2.97465	13.94	2.97762 ± 4.30E-05	139.86651 ± 4.16E-04	4.113	10.770
49	102756466	E1 3987	101.230	−0.86304	15.48	16.76987 ± 2.93E-01	151.94809 ± 1.26E-01	6.752	6.785
50	102779171	E1 1499	101.357	−1.06390	13.44	11.33939 ± 3.72E-02	143.75596 ± 1.34E-01	7.545	2.000

Table A.1. continued.

No.	CoRoT-ID	Win-ID	Alpha (°)	Delta (°)	*V* Mag	Period (d)	Epoch (d) +2 454 000	Dur. (h)	Depth (%)
51	102738614	E1 0827	101.130	−1.17246	14.45	7.76844 ± 5.16E-02	135.81384 ± 1.46E-01	3.511	17.555
52	102818537	E2 2620	101.631	−2.85605	14.45	2.27296 ± 4.80E-05	139.72413 ± 6.41E-04	5.438	9.254
53	102820928	E2 4500	101.648	−2.61561	16.16	1.82502 ± 1.77E-04	138.45024 ± 3.15E-03	3.848	4.915
54	102867757	E2 4431	101.947	−2.68001	16.11	2.68580 ± 2.89E-04	140.21954 ± 3.46E-03	2.552	8.510
55	102708916	E1 0484	100.957	−0.79757	13.97	6.18906 ± 6.35E-02	141.10739 ± 3.44E-01	5.335	21.340
56	102726405	E1 0801	101.061	−1.37603	12.76	2.54204 ± 2.90E-05	138.05727 ± 3.47E-04	4.280	18.720
57	102732394	E1 1251	101.095	−1.42804	14.96	1.57360 ± 4.30E-05	135.74521 ± 9.19E-04	3.056	6.810
58	102733170	E1 1543	101.100	−1.61003	13.68	1.97940 ± 4.50E-05	135.86023 ± 7.68E-04	3.949	3.770
59	102734453	E1 2507	101.107	−0.67484	14.47	8.37056 ± 6.80E-05	144.18882 ± 3.35E-03	21.700	8.371
60	102735868	E1 3810	101.115	−1.33074	15.25	1.64709 ± 1.80E-05	135.56796 ± 2.15E-03	3.775	9.000
61	102741994	E1 2336	101.149	−1.64399	14.47	4.62211 ± 1.07E-04	135.78605 ± 7.22E-04	4.124	9.500
62	102752408	E1 3080	101.207	−1.12243	16.13	21.26057 ± 5.41E-03	146.95066 ± 6.96E-03	4.600	1.525
63	102754263	E1 3846	101.217	−1.05010	15.31	2.45716 ± 1.50E-04	136.94466 ± 1.78E-03	2.994	7.260
64	102756903	E1 4392	101.232	−1.44495	15.90	0.97909 ± 1.50E-05	136.17055 ± 4.74E-04	2.418	3.070
65	102757626	E1 0791	101.236	−1.23750	14.70	1.20543 ± 6.10E-05	135.91488 ± 1.60E-03	3.441	9.600
66	102764398	E2 3602	101.275	−2.81121	16.23	0.92744 ± 5.00E-04	138.08047 ± 1.00E-04	2.702	4.689
67	102768859	E2 4148	101.300	−2.81762	16.10	8.06342 ± 5.26E-04	141.27802 ± 5.80E-03	4.913	1.444
68	102773399	E1 2875	101.326	−0.95011	14.81	0.60560 ± 1.00E-04	135.51522 ± 7.15E-03	2.702	3.850
69	102774523	E1 1052	101.332	−1.85324	14.89	5.91776 ± 1.09E-04	135.67799 ± 5.51E-04	3.901	27.240
70	102776173	E2 1176	101.341	−3.21882	14.90	0.72508 ± 5.00E-05	138.59908 ± 5.00E-04	2.702	3.240
71	102776386	E2 1137	101.342	−2.86191	13.50	2.20677 ± 2.70E-04	139.42573 ± 3.74E-03	3.684	3.570
72	102776565	E2 2143	101.343	−3.15951	14.63	2.20584 ± 6.50E-05	140.76363 ± 8.51E-04	4.111	56.400
73	102776605	E1 3357	101.344	−0.65412	16.23	2.18327 ± 5.20E-05	137.38286 ± 7.53E-04	4.109	59.790
74	102783117	E1 1002	101.379	−0.66941	14.88	0.78215 ± 1.00E-04	135.29534 ± 1.16E-03	2.702	0.430
75	102785724	E1 2613	101.394	−1.57614	15.88	4.71634 ± 6.50E-05	139.61223 ± 4.28E-04	5.267	23.860
76	102790392	E2 1005	101.421	−2.46922	14.72	4.91014 ± 9.90E-05	139.89439 ± 5.78E-04	5.419	15.410
77	102793963	E1 3124	101.441	−1.62531	16.19	1.24225 ± 1.00E-04	135.40128 ± 5.95E-04	1.596	2.070
78	102802054	E2 4445	101.506	−2.33150	15.96	2.12884 ± 1.69E-04	140.44080 ± 2.20E-03	2.540	2.440
79	102803023	E1 4206	101.514	−0.64875	15.69	2.32061 ± 6.00E-05	137.82606 ± 8.25E-04	4.263	15.620
80	102806377	E2 0836	101.541	−2.03210	13.13	3.81666 ± 3.70E-03	142.04834 ± 2.16E-02	4.222	13.380
81	102806577	E2 1918	101.543	−3.23352	14.24	3.66704 ± 3.20E-04	140.43028 ± 2.57E-03	4.925	16.500
82	102809393	E2 0486	101.566	−2.83432	14.08	7.71063 ± 4.54E-02	139.08695 ± 5.58E-02	6.247	7.470
83	102811578	E2 0416	101.582	−1.98315	12.47	1.66868 ± 1.25E-04	139.03337 ± 2.25E-03	2.782	2.800
84	102813089	E1 4561	101.592	−0.99226	16.24	1.30626 ± 3.90E-05	136.71588 ± 9.15E-04	3.026	23.100
85	102816070	E2 2295	101.613	−2.31198	15.63	7.44703 ± 2.65E-04	140.40955 ± 8.91E-04	6.238	25.550
86	102818428	E2 1307	101.630	−2.24680	13.79	7.45491 ± 4.48E-04	142.37746 ± 1.54E-03	6.238	5.520
87	102819360	E2 3054	101.636	−2.86079	15.15	0.99596 ± 5.00E-04	138.59319 ± 5.60E-03	2.812	3.730
88	102819692	E1 3127	101.638	−1.59328	15.86	1.38268 ± 2.10E-05	136.22874 ± 4.95E-04	3.462	30.170
89	102824749	E1 1971	101.675	−0.75888	14.28	8.09754 ± 2.55E-04	139.29042 ± 9.48E-04	6.403	22.900
90	102826984	E1 3686	101.691	−0.68487	15.10	1.47677 ± 1.40E-05	136.83385 ± 3.55E-04	3.046	26.680
91	102828417	E2 1036	101.701	−2.04626	14.80	9.59460 ± 2.66E-04	147.32365 ± 7.26E-04	6.453	14.340
92	102835452	E2 4071	101.748	−2.22388	15.71	6.93290 ± 7.68E-03	139.00417 ± 1.69E-02	5.080	50.780
93	102836138	E1 0844	101.753	−1.34797	14.72	3.55818 ± 4.90E-05	137.20937 ± 3.67E-04	3.922	16.770
94	102836169	E2 4009	101.753	−2.56595	16.16	1.18554 ± 5.00E-05	139.23407 ± 1.40E-03	1.874	24.690
95	102840080	E2 3619	101.779	−2.93765	15.38	2.33737 ± 1.93E-04	139.61448 ± 2.40E-03	2.557	2.180
96	102841939	E1 5038	101.791	−0.55531	16.02	2.37762 ± 3.60E-05	135.82534 ± 4.82E-04	3.983	29.670
97	102842120	E2 3952	101.792	−2.95054	14.17	1.10449 ± 3.90E-05	138.62653 ± 1.13E-03	3.285	38.860
98	102842466	E1 3571	101.795	−1.03743	14.42	4.91740 ± 5.04E-04	138.74857 ± 2.86E-03	5.419	67.290
99	102844991	E1 3252	101.812	−0.91820	15.99	1.07425 ± 1.80E-05	135.53889 ± 5.45E-04	2.428	15.620
100	102849348	E2 2452	101.840	−2.82048	14.79	1.81837 ± 5.60E-05	138.60443 ± 9.44E-04	3.223	10.440
101	102851363	E2 3081	101.852	−2.25781	15.67	1.01078 ± 2.10E-05	139.00262 ± 6.33E-04	2.419	22.270
102	102852229	E2 0872	101.858	−2.77432	13.31	6.06061 ± 3.82E-02	140.73996 ± 1.83E-01	5.756	9.680
103	102858100	E2 2099	101.892	−3.07796	14.46	1.31134 ± 9.00E-05	138.64401 ± 2.12E-03	3.311	4.330
104	102870155	E2 4907	101.961	−2.81992	16.20	2.78294 ± 8.40E-05	139.98194 ± 8.08E-04	4.440	15.050
105	102870613	E2 0117	101.964	−2.68863	12.54	7.13947 ± 4.85E-04	145.98116 ± 1.75E-03	6.084	41.650
106	102870852	E2 0609	101.965	−2.90340	14.26	0.76471 ± 5.20E-04	138.56904 ± 1.89E-03	2.844	2.500
107	102872646	E2 0818	101.976	−2.72664	14.40	1.88286 ± 4.17E-04	138.92797 ± 6.80E-05	3.940	4.350
108	102879375	E2 0365	102.017	−2.09075	13.67	0.97728 ± 5.00E-04	138.77715 ± 3.43E-03	3.129	6.730
109	102882044	E1 3079	102.033	−0.48467	16.08	9.07345 ± 5.60E-05	136.91781 ± 1.80E-05	4.127	28.910

Table A.1. continued.

No.	CoRoT-ID	Win-ID	Alpha (°)	Delta (°)	*V* Mag	Period (d)	Epoch (d) +2 454 000	Dur. (h)	Depth (%)
110	102884662	E1 1938	102.048	−1.00089	15.93	3.84822 ± 2.16E-04	138.97463 ± 1.73E-03	4.935	35.770
111	102886012	E1 4690	102.056	−1.61420	16.34	1.58466 ± 2.52E-04	136.15763 ± 4.04E-03	2.631	0.810
112	102889458	E1 4646	102.075	−1.00521	16.30	2.01989 ± 3.30E-05	136.31380 ± 5.05E-04	3.953	22.100
113	102892869	E1 3024	102.093	−0.56110	15.08	4.07590 ± 6.59E-04	139.53177 ± 5.41E-03	3.810	1.589
114	102896719	E1 3444	102.114	−0.47842	14.90	1.23114 ± 1.10E-04	135.97699 ± 2.98E-03	3.444	2.090
115	102900859	E1 1220	102.135	−0.53002	13.42	4.85346 ± 1.48E-04	136.52903 ± 8.29E-04	5.416	11.250
116	102902696	E1 1276	102.145	−0.75803	13.58	1.98087 ± 1.40E-05	136.66216 ± 2.41E-04	3.665	26.510
117	102914654	E2 4083	102.206	−2.15859	15.95	1.20531 ± 1.80E-05	139.12553 ± 4.68E-04	3.441	20.550
118	102929837	E2 1064	102.283	−2.89422	14.82	3.81996 ± 4.10E-05	139.41564 ± 3.47E-04	4.934	37.900
119	102930316	E2 2382	102.286	−2.95754	15.74	1.49577 ± 1.26E-04	139.76033 ± 2.53E-03	3.617	5.110
120	102931335	E1 3946	102.291	−1.44787	15.47	3.97923 ± 2.90E-05	138.84505 ± 2.29E-04	4.516	25.390
121	102932176	E2 1219	102.295	−1.99175	13.71	0.87225 ± 1.30E-05	139.05420 ± 2.29E-04	2.987	21.190
122	102943073	E2 0151	102.349	−2.48166	12.88	1.64410 ± 7.50E-05	139.62393 ± 1.34E-03	2.921	4.320
123	102955089	E2 1261	102.408	−1.83831	14.95	0.57161 ± 1.70E-05	138.98060 ± 3.17E-04	2.702	30.420
124	102961237	E2 3896	102.439	−2.56702	15.58	1.02102 ± 6.40E-05	139.41378 ± 1.77E-03	3.132	4.220
125	102965963	E2 4756	102.467	−2.16127	15.71	1.90365 ± 3.30E-05	140.09132 ± 4.99E-04	3.942	16.660
126	102980178	E2 4236	102.550	−2.68934	15.73	5.05476 ± 1.04E-03	139.07148 ± 4.98E-03	5.426	46.710
127	102983538	E2 2825	102.570	−2.93102	15.01	1.45435 ± 1.20E-04	139.03886 ± 2.39E-03	3.612	6.330
128	102801922	E1 0617	101.505	−1.50686	14.43	5.45907 ± 4.20E-05	138.93015 ± 2.32E-03	3.503	0.895
129	102927840	E2 4136	102.273	−2.66893	14.56	10.29535 ± 8.58E-03	140.69140 ± 1.81E-02	7.055	0.600
130	102726103	E1 0830	101.060	−1.22901	14.54	3.81466 ± 2.20E-05	137.99633 ± 1.82E-03	1.894	0.565
131	102786821	E1 2938	101.400	−1.32339	14.71	1.91876 ± 1.88E-04	135.51978 ± 3.41E-03	2.969	0.730
132	102802298	E2 4626	101.508	−2.45497	15.51	3.71918 ± 5.20E-05	139.05857 ± 4.08E-04	3.578	10.590
133	102932955	E2 2046	102.299	−2.76750	15.49	24.25906 ± 4.75E-04	140.53257 ± 5.33E-04	3.960	6.960
134	102806484	E2 4826	101.542	−2.71639	16.18	9.56081 ± 4.90E-05	140.53819 ± 1.38E-03	2.729	1.585
135	102735257	E1 3236	101.111	−1.635940	16.12	23.6935± 5.00e-04	156.952 ± 5.00e-04	4.265	11.6
136	102937382	E2 4533	102.322	−1.909260	15.02	7.69724 ± 3.89E-03	139.15290 ± 1.38E-03	6.247	0.170
137	102734591	E1 0663	101.107	−1.291500	14.39	8.16270 ± 6.13E-03	139.34211 ± 2.35E-02	6.400	0.100
138	102751150	E2 0193	101.200	−2.087960	13.07	6.34015 ± 1.50E-03	144.05301 ± 6.23E-03	5.910	0.160
139	102805003	E2 2539	101.530	−1.548410	14.54	5.57236 ± 6.45E-03	136.21190 ± 2.65E-03	13.800	0.110
140	102765275	E1 2060	101.280	−0.671730	15.55	–	177.43000 ± 1.00E-02	7.200	6.200
141	102829388	E2 3914	101.708	−3.030360	15.50	–	163.86000 ± 1.00E-02	18.400	8.500
142	102855409	E2 1633	101.877	−2.299030	13.18	–	155.43000 ± 1.00E-02	20.260	17.200
143	102868004	E2 2416	101.949	−2.206550	15.72	–	172.54000 ± 1.00E-02	5.750	5.700
144	102919036	E1 4818	102.229	−1.072490	15.69	–	174.45000 ± 1.00E-02	17.800	1.800
145	102801672	E2 4912	101.503	−2.599640	16.34	–	138.18000 ± 1.00E-02	9.070	8.200